Cloud to IDA: a very efficient solution for performing Incremental Dynamic Analysis

Cloud to IDA: una soluzione efficace per implementare un'analisi dinamica incrementale

A. Miano[1], F. Jalayer[1], A. Prota[1]

[1] *Department of Structures for Engineering and Architecture, University of Naples "Federico II"*

ABSTRACT: Incremental dynamic analysis (IDA) is a procedure in which a structure is subjected to a suite of ground motion records, scaled to multiple levels of intensity and leading to corresponding curves of response versus intensity. However, implementation of IDA usually involves a significant computational effort. In this work, a simple and efficient solution for IDA analysis with only few points, based on the structural response to un-scaled records (a.k.a the "cloud"), has been implemented. The transverse frame of a shear-critical seven-storey older RC building in Van Nuys, CA, which is modeled in Opensees with fiber-section considering the flexural-shear-axial interactions and the bar slip, is employed. It is demonstrated that the simplified IDA, obtained based on a significantly lower computational effort with respect to the full IDA, provides reliable results in terms of the statistics of structural response (e.g., mean and mean plus/minus one standard deviation) versus intensity and structural fragility. / L'analisi dinamica incrementale (IDA) è una procedura in cui una struttura è soggetta a una serie di accelerogrammi, scalati a differenti livelli di intensità, che portano a corrispondenti curve di risposta strutturale data l'intensità. L'implementazione di un'analisi IDA comporta un notevole onere computazionale. In questo lavoro, una soluzione semplice ed efficace per un'analisi IDA con soli pochi punti, scelti a partire dalla risposta strutturale ottenuta da accelerogrammi non scalati (metodo "cloud"), è stata implementata. Un telaio trasversale, critico a taglio, di un edificio esistente in C.A. di sette piani, sito in California, modellato in Opensees con sezioni a fibre, considerando l'interazione flessione-taglio-sforzo assiale ed il fenomeno del "bar slip", è utilizzato come caso studio. L'analisi IDA semplificata, nonostante un onere computazionale significativamente inferiore rispetto alla IDA classica, fornisce risultati affidabili in termini di statistiche della risposta strutturale (media e media più/meno dispersione) data l'intensità ed in termini di fragilità sismica.

KEYWORDS: seismic fragility, existing RC frames, non-linear dynamic analysis procedures/fragilità sismica, edifici esistenti in C.A., analisi dinamiche non lineari

1 INTRODUCTION

Many existing reinforced concrete (RC) moment-resisting frame buildings in regions with high seismicity were built without adequate seismic-detailing requirements and are particularly collapse-prone buildings. Identifying accurately the level of performance can facilitate an efficient seismic assessment and classification of these buildings. In this context, analytic structural fragility assessment is one of the fundamental steps in the modern performance-based engineering (Cornell & Krawinkler 2000). The structural fragility can be defined as the conditional probability of exceeding a prescribed limit state given the intensity measure (IM). There are alternative non-linear dynamic analysis procedures available in the literature for characterizing the relationship between engineering demand parameters (EDPs) and IM based on recorded ground motions, such as, the Incremental Dynamic Analysis (IDA, (Vamvatsikos & Cornell 2004) Multiple-Stripe Analysis (MSA, see (Jalayer & Cornell 2009)) and the Cloud Method (Bazzurro et al. 1998, Cornell et al. 2002, Jalayer 2003, Jalayer & Cornell 2003, Jalayer et al. 2015). The nonlinear dynamic methods such as IDA and MSA are suitable for evaluating the relationship between EDP and IM for a wide range of IM values; however, their application can be quite time-consuming as the non-linear dynamic analyses are going to be repeated (usually for scaled ground motions) for increasing levels of IM.

In this context, it can be very useful to find a way to reduce the computational effort of IDA analysis, keeping the same accuracy of the results. Herein, an alternative and more quick way to implement IDA analysis is presented, starting from the results of *Cloud Analysis*. Cloud analysis is based on a simple regression in the logarithmic space of the structural response versus the seismic intensity for a set of registered records. Cloud is particularly useful and efficient since it involves the non-linear analysis of the structure subjected to a set of un-scaled ground motions. It is shown herein that, exploiting the cloud results in term of predicted median and standard deviation, the IDA analysis can be performed in an efficient manner without significant loss of accuracy (with respect to a complete IDA). This method,

which is called *Cloud to IDA*, considers only few spectral acceleration levels (i.e., data points) for each record.

As a numerical example, the transverse frame of a seven-story existing RC building in Van Nuys, CA, modeled in Opensees modeled by considering the flexural-shear-axial interactions in the columns, is employed. Because of the old construction philosophy, column members are sensible to possible shear failure during earthquakes; hence, a non-linear model is used to predict an envelope of the cyclic shear response (Setzler & Sezen 2008, Sezen 2008). This envelope includes the shear displacements and corresponding strength predictions at the peak strength, onset of lateral strength degradation, and loss of axial-load-carrying capacity. In addition, the total lateral displacement of the members includes also the consideration of the deformability due to bar slip contribution. The adopted engineering demand parameter (EDP) is the critical demand to capacity ratio (Jalayer et al. 2007) corresponding to the component or mechanism that leads the structure closest to the onset of near collapse limit state. This structural response parameter, that is equal to unity at the onset of the desired limit state, can encompass both ductile and fragile failure mechanisms.

It is demonstrated that, for the case-study structure considered, the *Cloud to IDA* procedure provides reliable results in terms of the capacity curves that are very close to those based on a complete IDA and with smaller computational effort.

2 METHODOLOGY

2.1 *Structural performance variable*

The EDP herein is taken to be the critical demand to capacity ratio (Jalayer et al. 2007, Jalayer et al. 2015) denoted as Y_{LS} and defined as the demand to capacity ratio for the component or mechanism that brings the system closer to the onset of limit state LS (herein, the near collapse limit state). The formulation is based on the cut-set concept (Ditlevsen & Madsen 1996), which is suitable for cases where various potential failure mechanisms (both ductile and fragile) can be defined a priori. Y_{LS}, which is always equal to unity at the onset of limit state, is defined as:

$$Y_{LS} = \max_{l}^{N_{mech}} \min_{j}^{N_l} \frac{D_{jl}}{C_{jl}(LS)} \quad (1)$$

where N_{mech} is the number of considered potential failure mechanisms; N_l the number of components taking part in the lth mechanism; D_{jl} is the demand evaluated for the jth component of the lth mechanism;

$C_{jl}(LS)$ is the limit state capacity for the jth component of the lth mechansim. The capacity values refer to the near collapse limit state in this work, but the procedure can be repeated for any other prescribed limit state. In the context of this work, the demand is expressed in terms of maximum chord rotation for the component, denoted as θ_{max}, and computed based on the nonlinear dynamic analysis. The component chord rotation capacity is denoted as $\theta_{ultimate}$ corresponding to the ultimate capacity of the member. In particular, $\theta_{ultimate}$ corresponds to the point on the softening branch of the force-deformation curve of the member, where a 20% reduction in the maximum strength takes place.

The possible failure mechanisms are associated to the limit state of near collapse ($Y_{near\ collapse} = Y$). They correspond to ductile or brittle failures of the columns, depending on whether the column is flexural or shear critical. $Y > 1$ for a column is achieved when $\theta_{demand} > \theta_{ultimate}$ where $\theta_{ultimate}$ for each element takes into account the flexural/axial behavior, the shear behavior and the deformation due to bar slip.

When predicting non-linear response of structures, it is necessary to account for the possibility that some records may cause global "Collapse"; i.e., very high global displacement-based demands or non-convergence problems in the analysis software. It is obvious that, $Y > 1$ for the limit state of near-collapse does not guarantee the exceedance of collapse limit state. Herein, the cases of collapse are identified explicitly by verifying the following criteria for structural collapse: 1) 50% +1 of the columns of only one floor have achieved θ_{axial} (Galanis & Moehle 2015), where θ_{axial} corresponds to the point associated with the complete loss of vertical-load carrying capacity of the component on the softening branch; 2) 10% of the maximum interstory drift between all the floors has achieved.

2.2 *Nonlinear dynamic analyses procedure*

In order to estimate the structural fragility, *Cloud, IDA* and *Cloud to IDA* analyses are adopted herein as alternative nonlinear dynamic analysis procedures. The cloud analysis is a procedure in which a structure is subjected to a set of ground motion records of different first-mode Sa(T) values. The cloud data encompasses pairs of ground motion IM (herein first-mode Sa(T)) and its corresponding structural performance variable Y (see Eq. 1) for each record. Cloud method provides estimates of the first two statistical moments (e.g., logarithmic mean and standard deviation) of the performance parameter Y given the first-mode spectral acceleration. Once the ground motion records are selected, they are applied

to the structure and the resulting $Y=D/C$ (demand over capacity ratio, as described above) is calculated. This provides a set of values that form the basis for the cloud-method calculations. The cloud data can be separated to two parts: (a) *NoC* data which correspond to that portion of the suite of records for which the structure does not experience "*Collapse*", (b) *C* data for which the structure leads to "Collapse". In order to estimate the statistical properties of the cloud response, with respect to *NoC* data, conventional linear regression (using least squares) is applied to the response on the natural logarithmic scale, which is the standard basis for the underlying log-normal distribution model. This is equivalent to fitting a power-law curve to the cloud response in the original (arithmetic) scale. This results in a curve that predicts the median drift demand for a given level of structural acceleration:

$$\eta_{Y|Sa,NoC}(Sa) = a \cdot Sa^b$$
$$\ln(\eta_{Y|Sa,NoC}(Sa)) = \ln(a) + b \cdot \ln(Sa) \quad (2)$$

where $ln(a)$ and b are linear regression constants. The logarithmic standard deviation $\beta_{Y|Sa,NoC}$ can be estimated as the root mean sum of the square of the residuals with respect to the regression prediction:

$$\beta_{Y|Sa,NoC} = \sqrt{\frac{\sum (\ln(Y_i) - \ln(a \cdot S_{a,i}{}^b))^2}{N_{NoC} - 2}} \quad (3)$$

where Y_i and $S_{a,i}$ are the demand over capacity ratio values and the corresponding spectral acceleration for record number i within the cloud response set and N_{NoC} is the number of *NoC* records.

The standard deviation of regression, as introduced in the preceding equation, is presumed to be constant with respect to spectral acceleration over the range of spectral accelerations in the cloud.
The fragility, expressed generally as the conditional distribution of Y given Sa, can be expanded with respect to *NoC* and *C* data as follows using Total Probability Theorem (see [Shome & Cornell 1999, Jalayer & Cornell 2009, Miano et al. 2017]):

$$P(Y > 1 | Sa) = P(Y > 1 | Sa, NoC) \cdot P(NoC | Sa)$$
$$+ P(C | Sa) \quad (4)$$

The probability terms in Eq. (4) are described clearly as follows:

❒ The *NoC* term $P(Y>1|Sa,NoC)$ is the conditional distribution of Y given Sa and *NoC*, and can be described by a lognormal distribution (a widely used assumption that has been usually verified for cases where the regression residuals represent unimodal behavior, see e.g. [Jalayer & Cornell 2009, Jalayer and Ebrahimian 2016, Miano et al. 2017]):

$$P(Y > 1 | Sa, NoC) = \Phi\left(\frac{\ln \eta_{Y|Sa,NoC}}{\beta_{Y|Sa,NoC}}\right) \quad (5)$$

where Φ is the standardized Gaussian cumulative distribution function (CDF) and $\eta_{Y|Sa,NoC}$ and $\beta_{Y|Sa,NoC}$ are presented in Eqs. (2) and (3). It should be noted that Eq. (4) is based on the implicit assumption that in the cases of global dynamic instability (global Collapse), the limit state LS (hereafter LS= Near Collapse) is certainly exceeded.

❒ The term $P(C|Sa)=1-P(NoC|Sa)$ is probability of global dynamic instability (Collapse), which can be expressed by a logistic regression model (a.k.a., logit) on the Sa values of the entire cloud data:

$$P(C | Sa) = \frac{1}{1 + e^{-(\beta_0 + \beta_1 \cdot Sa)}} \quad (6)$$

where β_0 and β_1 are the parameters of the logistic regression. It is to note that the logistic regression model belongs to the family of generalized regression models and is particularly useful for cases in which the regression dependent variable is binary (i.e., can have only two values 1 and 0, *yes* or *no*, which is the case of *C* and *NoC* herein). Note that the logistic regression model described above is applied to all records; they are going to be distinguished by 1 or 0 depending on whether they lead to *C* or *NoC*.

The structural fragility from IDA analysis can be calculated using the (Log-Normal) probability density function fitted to the spectral acceleration values at $Y=1$, $Sa_{Y=1}$:

$$P(Y > 1 | Sa) = P(Sa_{Y=1} < Sa) = \Phi\left(\frac{\ln Sa - \ln \eta_{Sa_{Y=1}}}{\beta_{Sa_{Y=1}}}\right) \quad (7)$$

where $\eta_{SaY=1}$ and $\beta_{SaY=1}$ are the parameters of the Log-Normal probability density function.

The proposed *Cloud to IDA* procedure can be carried out by considering few levels of spectral acceleration for each record (limited to 4 levels in the majority of cases), in order to obtain the distribution of $Sa_{Y=1}$. In particular, four spectral acceleration levels are chosen per record based on the results of cloud analysis; namely, the original $Sa(T_1)$; median $S_a(T_1)$ at $Y=1$ estimated based on Cloud Analysis (equal to $(1/a)^{1/b}$ per Eq. (2)); (logarithmic) mean plus one standard deviation $S_a(T_1)$ at $Y=1$ estimated based on Cloud Analysis (equal to $(1/a)^{1/b} e^{+\beta_{Y|Sa,NoC}}$ per Eqs. (2) and (3)); and (logarithmic) mean minus one standard deviation $S_a(T_1)$ at $Y=1$ (equal to $(1/a)^{1/b} e^{-\beta_{Y|Sa,NoC}}$ per Eqs. (2) and (3)). Obviously, other scaling points can be added as needed, by assigning a certain value of α in order to calculate (logarithmic) mean plus or minus α standard deviation

$S_a(T_1)$ at Y=1 estimated based on Cloud AnalysiS equal to $(1/a)^{1/b} \, e^{\pm\alpha\beta_{Y|Sa,NoC}}$. As a rule of thumb, it is important to have enough spectral acceleration levels so that the resulting IDA curve (obtained by connecting the points) covers Y=1 (that is, $Sa_{Y=1}$ for each record can be obtained by interpolation). Finally, the structural fragility from *Cloud to IDA* analysis is calculated the same as that of IDA analysis (see Eq. 7).

3 NUMERICAL APPLICATION

3.1 *Building description and modeling*

One of the transverse frames of the seven-story hotel building in Van Nuys, California, is modeled and analyzed in this study. The building is located in the San Fernando Valley of Los Angeles County (34.221° north latitude, 118.471° west longitude). The frame building was designed in 1965 according to the 1964 Los Angeles City Building Code, and constructed in 1966. The building was severely damaged in the M6.7 1994 Northridge earthquake (Krawinkler 2005).

Columns in the transverse frame are 356 mm wide by 508 mm deep, i.e., oriented to bend in their strong direction when resisting lateral forces in the plane of the transversal frame. Spandrel beams in the frame are typically 406 mm wide and 762 mm deep in the second floor, 406 mm wide and 572 mm deep in the third through seventh floors, and 406 mm by 559 mm at the roof level. Column concrete has compressive nominal strength *f'c* of 34.5 MPa in the first story, 27.6 MPa in the second story, and 20.7 MPa in other floors. Beam and slab concrete strength *f'c* is 27.6 MPa in the second floor and 20.7 MPa in other floors. Grade 60 (*fy*=414 MPa) reinforcing steel is used in columns. The specified yield strength, *fy*, is 276 MPa (Grade 40) for the steel used in beams and slabs. The column and beam reinforcement details are provided in Krawinkler (2005). Figure 1 shows the transverse frame modeled in this research.
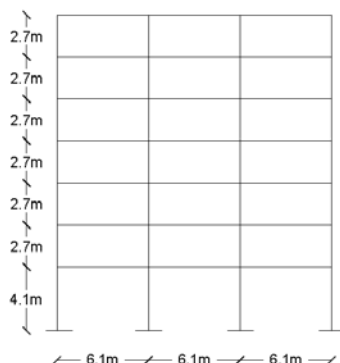

Figure 1. Geometric configuration of the transverse frame.
Configurazione geometrica del telaio trasversale.

3.1.1 *Flexural, shear and bar slip models*

The Holiday Inn hotel building experienced multiple shear failures in the columns in the fourth story during the 1994 Northridge earthquake (Krawinkler 2005) in the longitudinal perimeter frames. The amount and the spacing of the transversal reinforcement in most columns were insufficient. Therefore, it is necessary to model materials and column members to capture the shear and the flexure-shear failure modes in columns and the potential collapse of the transverse frame. About flexural model, unidirectional axial behaviour of concrete and steel are modeled to simulate the nonlinear response of beams and columns. Concrete material response is simulated using the Concrete01 material in OpenSees (http://opensees.berkeley.edu), which includes zero tensile strength and a parabolic compressive stress-strain behaviour up to the point of maximum strength with a linear deterioration beyond peak strength. Because the transverse reinforcement ratio for beams and columns in the Van Nuys building is relatively low and detailing does not meet the modern seismic code requirements, concrete is modeled more close to the unconfined model, with peak strength achieved at a strain of 0.002 and minimum post-peak strength achieved at a compressive strain of 0.006. The corresponding stress capacity at ultimate strain is 0.05*f'c for *f'c*=34.5MPa and for *f'c*=27.6MPa and 0.2*f'c for *f'c*=20.7MPa. Longitudinal reinforcing steel behavior is simulated using the Steel02 material in OpenSees. This model includes a bilinear stress-strain envelope with a curvilinear unload-reload response under cyclic loading. The previous research indicate that the observed yield strength of reinforcing steel exceeds the nominal strength (Krawinkler 2005, Islam 1996). As suggested by Islam (1996), yield strength of 345 MPa (50 ksi) and 496 MPa (72 ksi) are used in this research for Grade 40 and Grade 60, respectively. Both Grade 40 and Grade 60 reinforcement are assumed to have a post-yield modulus equal to 1% of the elastic modulus, which is assumed to be 200 GPa. Additional parameters required to define the Steel02 material model are taken equal to those recommended in the OpenSees User's Manual.

Flexural response of beams and columns response is simulated using fiber cross sections, representing the beam-column line elements. Uniaxial fibers within the gross cross section were assigned either concrete or steel. A typical column cross section included 30 layers of axial fibers, parallel to the depth of the section. In OpenSees, flexural beam-column members are modeled as force-based in which a specific moment distribution is assumed along the length of the member. An internal element solution

is required to determine member deformations that satisfy the system compatibility. In force-based column elements, distributed plasticity model is used in OpenSees in order to allows for yielding and plastic deformations at any integration point along the element length under increasing loads. In order to characterize the numerical integration options for the force-based column element and to accurately capture plastic deformations along the members, Newton-Cotes integration (Scott & Fenves 2006) is selected. Newton-Cotes method distributes integration points uniformly along the length of the element, including one point at each end of the element (Figure 2a). Beams member force-deformation response is computed assuming that inelastic action occurs mainly at the member ends and that the middle of the member remains typically elastic, but this is not necessary. Plastic hinge integration methods are used to confine non linear deformations in end regions of the element of specified length. The remainder of the element is assumed to stay linear elastic and it is assumed that the length of plastic region is equal to the depth of the cross-section. The modified Gauss Radau hinge integration method is used for numerical integration to capture non linear deformations near the ends of the force-based beam elements. The modified two-point Gauss-Radau integration within each hinge region is implemented at two integration points at the element ends and at 8/3 of the hinge length, $Lo=h$, from the end of the element (Figure 2b).

As far as it regard shear modeling, the shear model by Setzler and Sezen (2008) can capture the shear response with a lateral force-shear displacement envelope, that includes three distinct points corresponding to: 1)Maximum shear strength and corresponding shear displacement; 2)Onset of shear strength degradation and corresponding displacement; 3)Shear displacement at axial load failure. The shear strength is calculated according to the model by Sezen and Moehle (2004):

$$V_n = V_s + V_c = k \frac{A_v f_y d}{s} +$$
$$+ k \left(\frac{0.5\sqrt{f_c}}{a/d} \sqrt{1 + \frac{P}{0.5\sqrt{f_c} A_g}} \right) 0.8 A_g \qquad (8)$$

where A_v is the transverse reinforcement area in the loading direction; s is the transverse reinforcement spacing; f_y is the transverse reinforcement yield strength; d is the section depth; f'_c is the compressive strength of concrete; a is the shear span of the element; P is the axial load; A_g is the gross area of the section; k is a factor to account for ductility-related strength degradation and it is defined to be

equal to 1.0 for displacement ductility less than 2, equal to 0.7 for displacement ductility exceeding 6, and varies linearly for intermediate displacement ductility values.

Shear displacements are calculated using a combination of two existing models (Sezen 2008 and Setzler and Sezen 2008). The shear displacement at peak strength, $\Delta_{v,n}$, is calculated as:

$$\Delta_{v,n} = \left(\frac{f_y \cdot \rho_l}{5000 \cdot \frac{a}{d} \cdot \sqrt{\frac{P}{A_g \cdot f'_c}}} - 0.0004 \right) \cdot L \qquad (9)$$

where ρ_l is the longitudinal steel ratio and L is the length of the column.

As described in Sezen 2008, the shear displacement at the onset of shear failure is adopted from Gerin & Adebar (2004). Shear displacement at axial failure is obtained using the procedure given in Setzler & Sezen 2008, which requires the calculation of total lateral displacement. Total lateral drift is calculated using the equation proposed by Elwood & Moehle (2004).

About bar slip model, when a reinforcing bar embedded in concrete is subjected to a tensile force, strain accumulates over the embedded length of the bar. This tensile strain causes the reinforcing bar to slip relative to the concrete in which it is embedded. Slip of column reinforcing bars at column ends (i.e., from the footing or beam-column joint) will cause rigid body rotation of the column. This rotation is not accounted for in flexural analysis, where the column ends are assumed to be fixed. The bar slip model used in this study was originally developed by Sezen & Moehle (2003) and presented in Setzler & Sezen (2008). This model assumes a stepped function for bond stress between the concrete and reinforcing steel over the embedment length of the bar. The bond stress is taken as $1 \cdot \sqrt{f'c}$ MPa for elastic steel strains and as $0.5 \cdot \sqrt{f'c}$ MPa for inelastic steel strains. The rotation due to slip, θ_s, is calculated as $slip/(d-c)$, where slip is the extension of the outermost tension bar from the column end and d and c are the distances from the extreme compression fiber to the centroid of the tension steel and the neutral axis, respectively. The column lateral displacement due to bar slip, Δ_{slip}, is equal to the product of the slip rotation and the column length ($\Delta_{slip} = \theta_s \cdot L$).

3.1.2 Total lateral response

The total lateral response of a RC column can be modeled using a set of springs in series in OpenSees (where the flexural spring is represented by a fiber section element). The flexure, shear and bar slip deformation models discussed above are each modeled

by springs in series. Each spring is subjected to the same lateral force. The total displacement response is the sum of the responses of each spring. The column spring model is shown in Figure 2. A typical column element includes two zero-length bar slip springs at its ends, one zero-length shear spring and a flexural element with five integration points. The shear behavior is modeled as an uniaxial hysteretic material defined for the spring in the shear direction (i.e., transverse direction of the column or direction 1 in figure 2). The longitudinal displacement caused by the bar slip is modeled with two rotational springs at the column ends using an uniaxial hysteretic material (i.e., direction 3 in Figure 2). Finally, same vertical displacement is maintained between nodes of zero length elements in the vertical direction (i.e., direction 2 in Figure 2), using the equal-DOF option in OpenSees.
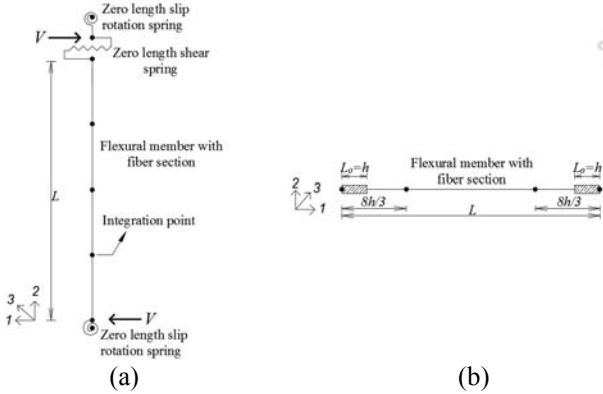
(a)   (b)

Figure 2. Elements used for modeling (a) columns and (b) beams. *Elementi usati per modellare (a) le colonne e (b) le travi.*

The three deformation components are simply added together to predict the total response up to the peak strength of the column (Setzler and Sezen 2008). Rules are established for the post-peak behavior of the springs based on a comparison of the shear strength V_n, the yield strength V_y, and the flexural strength V_p required to reach the plastic moment capacity. By comparing V_n, V_y, and V_p, the columns can be classified into five different categories, as described in Setzler and Sezen (2008): 1) Category I: $V_n<V_y$: the shear strength is less than the lateral load causing yielding in the tension steel. The column fails in shear while the flexural behavior remains elastic; 2) Category II: $V_y<V_n<0.95\cdot V_p$: the shear strength is greater than the yield strength, but less than the flexural strength of the column. The column fails in shear, but inelastic flexural deformation occurring prior to shear failure affects the post-peak behavior; 3) Category III: $0.95\cdot V_p<V_n<1.05\cdot V_p$: the shear and flexural strengths are very close; 4) Category IV: $1.05\cdot V_p<V_n<1.4\cdot V_p$: the shear strength is greater than the flexural strength of the column. The column experiences large flexural deformations po-

tentially leading to a flexural failure. Inelastic shear deformations affect the post-peak behavior, and shear failure may occur as displacements increase; 5) Category V: $V_n<1.4\cdot V_n$: the shear strength is much greater than the flexural strength of the column. The column fails in flexure while the shear behavior remains elastic. Figure 3 shows the three different deformation components and the total lateral displacement for two generic columns of the frame, belonging to two different categories.
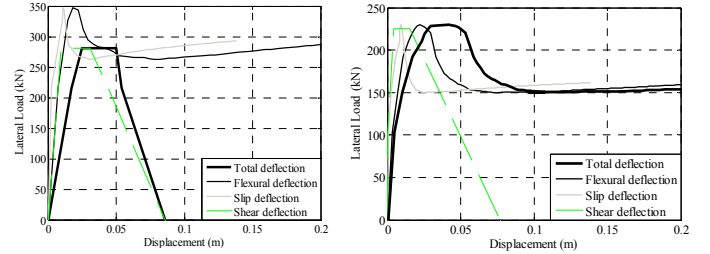
Figure 3. Three different deformation components and the total lateral displacement for two generic columns of the frame, belonging to Category I (left) and Category III (right). *Le tre differenti componenti deformazionali e la risposta laterale totale per due generiche colonne del telaio, appartenenti alle categorie I (sinistra) e III (destra).*

3.2 Record selection

A set of 34 strong ground-motion records are selected from the NGA-West2 database (Ancheta et al. 2014). This suite of records covers a wide range of magnitudes between 5.5 and 7.9, and closest distance-to-ruptured area (denoted as RRUP) up to around 40 km. Since the soil shear wave velocity in upper 30m of soil, Vs30, at the structure's site is around 218 m/sec, all selected records are chosen to be on NEHRP site classes C-D (where C:*360< Vs30<760 m/s* and D:*180< Vs30≤360 m/s*). The number of records from a single seismic event is limited to one, while only one of the two horizontal components of each recording, with higher spectral acceleration around 1.0 sec, is selected. The lowest useable frequency of 0.25Hz ensures that the low-frequency content is not removed by the ground motion filtering process. The records are selected to be free field or on the ground level without consideration of station housing.

3.3 Cloud analysis

As explained comprehensively in section 2.2, the Cloud Analysis is a nonlinear dynamic procedure in which the structure is subjected to a set of (un-scaled) ground motion records covering a wide range of IM, herein $Sa(T_1)$, values. Fig. 4 shows the Cloud data and the associated Cloud linear regression (fitted to the *NoC* portion of the Cloud data). For each data point (colored squares), the corre-

sponding record ID is shown. It can be see that 7 records out of 34 ground motions cause collapse or global dynamic instability (*C* data) as shown with red-colored squares. The line *Y*=1 corresponding to the onset of Near Collapse LS is shown with dashed red line.
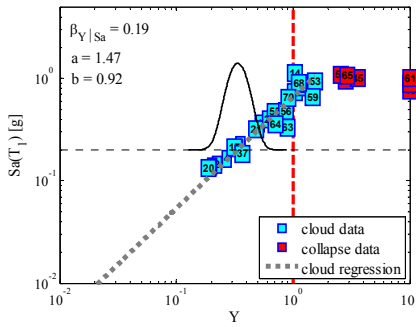

Figure 4. The Cloud Regression. Regressione della Cloud.

3.4 *IDA analysis*

Each IDA curve herein shows the variation in the performance variable *Y* for a given ground motion record as a function of $Sa(T_1)$ while the record is scaled-up linearly in amplitude. Each IDA curve has 19 strips. Initially a constant step of 0.1 from 0.1g to 1.5g has been adopted. Since the goal is that all IDA curves are able to populate both the *Y<1* and *Y>1* zones (for the purpose of interpolation of $Sa_{Y=1}$), the records are scaled to four spectral acceleration levels (see the methodology section, in reality one of the levels correspond to the unscaled spectral acceleration). It can be seen that these spectral acceleration levels cover values ranging between 0.4g and 0.8g (the zone in which most of the records exceed *Y=1*). Fig.5 illustrates the complete IDA curves (in thin grey lines) with respect to *Y* for the suite of 34 ground-motions. The vertical red line plotted at *Y*=1 demonstrates the dispersion in the spectral acceleration values $Sa_{Y=1}$ plotted as red-star points. The figure also demonstrates the (Log-Normal) probability density function fitted to the $Sa_{Y=1}$ values. The horizontal red-dashed line represents the median of $Sa_{Y=1}$ values (denoted as $\eta_{SaY=1}$) from IDA analysis. In order to facilitate the comparison with Cloud Analysis results, the corresponding Cloud data (the squares) and the regression prediction (blue line) are also plotted. The spectral acceleration value corresponding to *Y*=1 from the Cloud regression prediction (derived as $\eta_{SaY=1} = (1/a)^{1/b}$, the blue dashed line) represents the median spectral acceleration capacity corresponding to Cloud analysis.
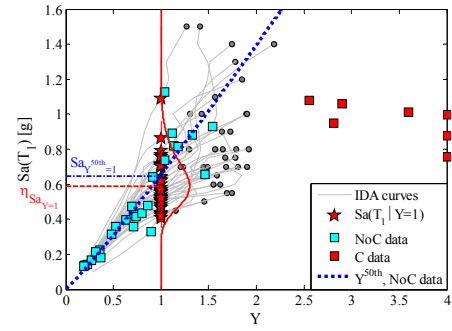

Figure 5. IDA curves, Cloud data, and the regression prediction. Curve IDA, dati e regressione della Cloud.

3.5 *Cloud to IDA*

As described in section 2.2, *Cloud to IDA* proposes an efficient procedure for performing IDA, which only considers few points (in most cases 4 points) of spectral acceleration for each record, in order to obtain the distribution of $Sa_{Y=1}$. Initially, all the records are scaled to the four points presented in section 2.2. Since, as said, the goal is that all the records are able to populate both the *Y<1* and *Y>1* zones for producing a good estimation of the distribution of $Sa_{Y=1}$. Just for four records, it was necessary to use a fifth level of scaling equal to $(1/a)^{1/b} \cdot e^{-2\sigma_{Y|Sa,NoC}}$. Figure 6 shows the *Cloud to IDA* results.
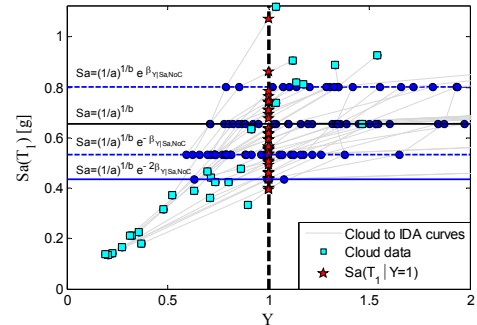

Figure 6. Cloud to IDA analysis. Analisi Cloud to IDA.

3.6 *Fragility curves results and comparisons*

Figure 7 illustrates a comparison between the three non-linear dynamic procedures (Cloud, *Cloud to IDA* and IDA) discussed herein. Table 1 shows the statistical parameters for the fragility curves, where η is the median value of the fragility curve and β is its standard logarithmic deviation.
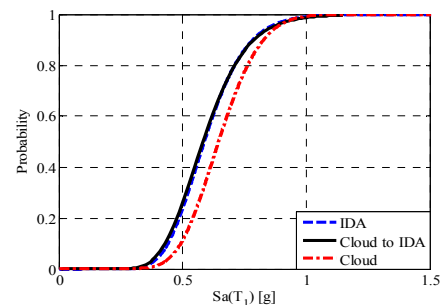

Figure 7. Fragility curves comparison. Confronto tra le curve di fragilità.

Table 1. Statistical parameters for fragility curves. Parametri statistici delle curve di fragilità.

Methodology	$\eta(g)$	β	Number of analyses
Cloud	0.65	0.21	34
IDA	0.59	0.22	19·34
Cloud-IDA	0.59	0.23	4·34+4

CONCLUSIONS

Cloud to IDA procedure is proposed herein as an efficient procedure for implementing incremental dynamic analysis (IDA), by exploiting both the data points and the statistic estimates from a simple Cloud Analysis. The transverse frame of a shear-critical seven-storey older RC building in Van Nuys, CA, which is modeled in Opensees with fiber-section considering the flexural-shear-axial interactions and the bar slip, is employed in order to illustrate this procedure. In particular, the procedure of *Cloud to IDA* manages to get the same results (in terms of fragility and for this specific case-study structure) as the complete IDA procedure based on only around 4 data point per ground motion record. La procedura Cloud to IDA è presentata come una soluzione efficiente per implementare un'analisi IDA. Essa si serve sia dei punti che delle stime statistiche di un'analisi Cloud. Il telaio trasversale di un edificio in C.A., sito in Van Nuys, CA, critico a taglio e modellato in OpenSees con sezioni a fibre e considerando l'interazione flessione-taglio-sforzo assiale ed il fenomeno del bar slip, è usato come caso studio. La procedura Cloud to IDA, basata solitamente su 4 punti riesce a cogliere gli stessi risultati di un'IDA completa in termini di curva di fragilità per il caso studio.

ACKNOWLEDGEMENTS

REFERENCES

Ancheta TD et al. NGA-West2 Database. Earthquake Spectra 2014; 30(3):989–1005.

Bazzurro P, Cornell CA, Shome N, Carballo JE (1998): Three proposals for characterizing MDOF nonlinear seismic response. Journal of Structural Engineering, 124(11), 1281-1289.

Cornell CA, Krawinkler H (2000): Progress and challenges in seismic performance assessment. PEER Center News, 3(2), 1-3.

Cornell CA, Jalayer F, Hamburger RO, Foutch DA (2002): The probabilistic basis for the 2000 SAC/FEMA steel moment frame guidelines. ASCE Journal of Structural Engineering, 128, 526–533, Special Issue: Steel Moment Resisting Frames after Northridge Part II.

Ditlevsen O, Madsen HO (1996): Structural reliability methods, Wiley, New York.

Elwood KJ, Moehle, JP (2005): Axial capacity model for shear-damaged columns. ACI Structural Journal 102, 578-587.

Galanis PH, Moehle JP (2015): Development of Collapse Indicators for Risk Assessment of Older-Type Reinforced Concrete Buildings. Earthquake Spectra, 31(4), 1991-2006.

Gerin M, Adebar P (2004): Accounting for shear in seismic analysis of concrete structures. 13th World Conference on Earthquake Engineering, Vancouver, B.C., Canada.

Jalayer F (2003): Direct Probabilistic seismic analysis: implementing non-linear dynamic assessments. Ph.D. dissertation, Stanford University, California.

Jalayer F, Cornell CA (2003): A technical framework for probability-based demand and capacity factor design (DCFD) seismic formats. Technical Report PEER 2003/08, Pacific Earthquake Engineering Research, Berkeley, USA.

Jalayer F, Franchin P, Pinto PE (2007): A scalar damage measure for seismic reliability analysis of RC frames. Earthquake Engineering & Structural Dynamics, 36(13), 2059-2079.

Jalayer F, Cornell CA (2009): Alternative non-linear demand estimation methods for probability-based seismic assessments. Earthquake Engineering & Structural Dynamics, 38(8), 951-972.

Jalayer F, De Risi R, Manfredi G (2015): Bayesian Cloud Analysis: efficient structural fragility assessment using linear regression. Bulletin of Earthquake Engineering, 13(4), 1183-1203.

Jalayer, F. and Ebrahimian, H., 2016. Seismic risk assessment considering cumulative damage due to aftershocks. Earthquake Engineering & Structural Dynamics (*In Press*).

Krawinkler H (2005): Van Nuys hotel building testbed report: exercising seismic performance assessment. Technical Report PEER 2005/11, Pacific Earthquake Engineering Research, Berkeley, USA.

Islam, M. S. (1996). "Analysis of the Northridge earthquake response of a damaged non-ductile concrete frame building." The structural design of tall buildings, 5(3), 151-182.

Miano A, Jalayer F, Ebrahimian H, Prota A, Manfredi G (2017): Cloud analysis considering global dynamic instability. 16th World Conference on Earthquake Engineering

Scott MH, Fenves GL (2006): Plastic hinge integration methods for force-based beam–column elements. Journal of Structural Engineering, 132(2), 244-252.

Setzler EJ, Sezen H (2008): Model for the lateral behavior of reinforced concrete columns including shear deformations. Earthquake Spectra, 24(2), 493-511.

Sezen, H., & Moehle, J. P. (2003). Bond-slip behavior of reinforced concrete members. In Proceedings of Fib Symposium on Concrete Structures in Seismic Regions.

Sezen H, Moehle JP (2004): Shear strength model for lightly reinforced concrete columns. Journal of Structural Engineering, 130(11), 1692-1703.

Sezen H (2008): Shear deformation model for reinforced concrete columns. Structural Engineering and Mechanics 28(1), 39-52.

Shome N, Cornell CA. Probabilistic seismic demand analysis of nonlinear structures. RMS Program, Stanford University 1999; Report No. RMS35, 320 pp.

Vamvatsikos D, Cornell CA (2004): Applied incremental dynamic analysis. Earthquake Spectra, 20(2), 523-553.